Synthesis and Biochemical Evaluation of *N*-(4-Phenylthiazol-2-yl)benzenesulfonamides as High-Affinity Inhibitors of Kynurenine 3-Hydroxylase

Stephan Röver,* Andrea M. Cesura, Philipp Huguenin,† Rolf Kettler, and Andre Szente

Pharma Division, Preclinical Research, Nervous System Diseases and Isotope Laboratory, F. Hoffmann-La Roche Ltd., CH-4070 Basel, Switzerland

Received July 17, 1997[⊗]

In this paper we describe the synthesis, structure−activity relationship (SAR), and biochemical characterization of *N*-(4-phenylthiazol-2-yl)benzenesulfonamides as inhibitors of kynurenine 3-hydroxylase. The compounds 3,4-dimethoxy-*N*-[4-(3-nitrophenyl)thiazol-2-yl]benzenesulfonamide **16** (IC_{50} = 37 nM, Ro-61-8048) and 4-amino-*N*-[4-[2-fluoro-5-(trifluoromethyl)phenyl]-thiazol-2-yl]benzenesulfonamide **20** (IC_{50} = 19 nM) were found to be high-affinity inhibitors of this enzyme in vitro. In addition, both compounds blocked rat and gerbil kynurenine 3-hydroxylase after oral administration, with ED_{50}'s in the 3−5 μmol/kg range in gerbil brain. In a microdialysis experiment in rats, **16** dose dependently increased kynurenic acid concentration in the extracellular hippocampal fluid. A dose of 100 μmol/kg po led to a 7.5-fold increase in kynurenic acid outflow. These new compounds should allow detailed investigation of the pathophysiological role of the kynurenine pathway after neuronal injury.

Introduction

Pharmacological control of the cascade of toxic events that lead to delayed neuronal cell death after stroke, brain trauma, or microbial and viral infections remains an unmet medical need. Research has centered on the excitotoxin hypothesis of neuronal injury. This hypothesis states that a massive release of excitotoxic amino acid neurotransmitters, mainly glutamate, from dying neurons aggravates the injury to the brain, in a vicious circle of glutamate released by dying neurons and concomitant Ca^{2+} influx into cells unaffected by the primary insult but not able to cope with the metabolic stress presented by excessively high intracellular Ca^{2+} levels.[1,2] Excellent tools, in particular potent antagonists at the *N*-methyl-D-aspartate (NMDA) class of glutamate receptors, have yielded insight into this pathological cascade. These compounds have been shown to be effective in animal models of stroke especially when given immediately after the insult.[3] At the same time, endogenous substances were discovered that exert neurotoxic or neuroprotective effects through glutamate receptors, including two metabolites of the kynurenine pathway[4] for the metabolism of L-tryptophan, namely kynurenic acid (KYNA) and quinolinic acid (QUIN). KYNA is an unselective glutamate receptor antagonist and has neuroprotective properties. It also blocks the glycine site of the NMDA receptor and has served as a lead compound in the development of glycine site antagonists.[5,6] QUIN on the other hand is an agonist at NMDA receptors and therefore neurotoxic.

Under physiological conditions QUIN and KYNA concentrations in brain tissues are low, possibly due to the low expression level and heterogeneous distribution of the kynurenine pathway enzymes. Recently, it has been shown that cerebral QUIN concentrations rise dramatically under pathological conditions which are accompanied by brain inflammation.[7,8] The rise in QUIN concentration can be attributed to several factors: (a) Indolamine 2,3-dioxygenase (IDO), the first enzyme of the pathway in nonhepatic tissues, is inducible by IFN-γ[9] and enzyme activity rises up to 30-fold in inflammatory brain tissue.[7,10] (b) Invading macrophages bring with them their enzymatic machinery to produce QUIN.[11] (c) Microglial cells will produce QUIN from L-tryptophan and/or kynurenine upon immune activation.[12] Studies done at the National Institute of Mental Health (NIMH) have shown that QUIN concentrations rise dramatically in some neuroinflammatory conditions in humans (AIDS-dementia complex) and that in different models of brain inflammation this rise in concentration closely follows the time course and severity of neurological impairment.[8,13−15] Evidence that this rise in QUIN concentration is causative for or contributes to the delayed neurological damage has been difficult to obtain due to the lack of potent and in vivo active inhibitors of the kynurenine pathway enzymes. Scientific debate has focused on QUIN concentrations measured in inflammation models vs those reported to be toxic in neuronal cell cultures instead. However, QUIN concentrations reported to be toxic in culture range from 0.1 μM after long-term exposure to 100 μM in an acute setting.[16−18]

Chart 1. Structures of Known Kynurenine 3-Hydroxylase Inhibitors

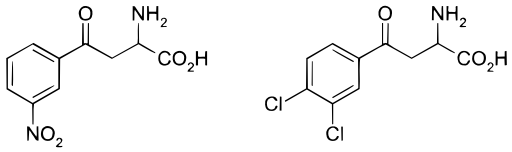

The scenario changed when in 1994 (*m*-nitrobenzoyl)-alanine (m-NBA)[19,20] and later FCE 28833[21] (Chart 1) were developed as inhibitors of kynurenine 3-hydroxylase and reported to have neuroprotective properties. Kynurenine 3-hydroxylase[22] has been chosen as target with the rational of decreasing QUIN concentration, concomitantly shunting the metabolism of kynurenine

† Isotope Laboratory.
[⊗] Abstract published in *Advance ACS Abstracts,* November 15, 1997.

S0022-2623(97)00467-6 CCC: $14.00

Scheme 1[a]

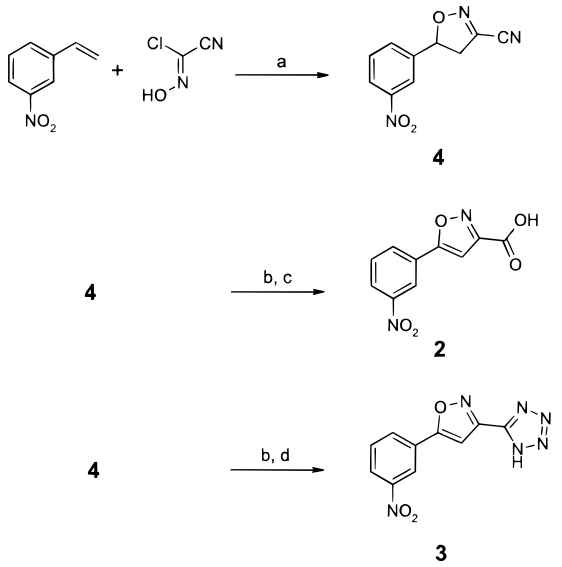

[a] Reagents: (a) sodium carbonate, room temperature; (b) *N*-bromosuccinimide, dibenzoyl peroxide, CCl_4, reflux; (c) sodium hydroxide, 50% ethanol, reflux; (d) sodium azide, ammonium chloride, DMF, 80 °C.

toward KYNA via kynurenine aminotransferase. Thus the neuroprotective properties observed with m-NBA and FCE 28833 have been ascribed, at least in part, to elevated KYNA levels.[21] However these compounds still may not be potent enough in vivo for an unequivocal assessment of the role of QUIN in animal models of delayed neurological damage.

Herein, we describe our efforts to identify inhibitors of kynurenine-3-hydroxylase using m-NBA and a screening hit, the sulfonamide **5**, as lead structures. This has resulted in the identification of 3,4-dimethoxy-*N*-[4-(3-nitrophenyl)thiazol-2-yl]benzenesulfonamide **16** and 4-amino-*N*-[4-[2-fluoro-5-(trifluoromethyl)phenyl]thiazol-2-yl]benzenesulfonamide **20**, compounds which possess high affinity and in vivo potency as inhibitors of kynurenine-3-hydroxylase. These new compounds should allow a more detailed assessment of the relevance of QUIN and other kynurenine pathway metabolites in animal models of neurological damage.

Chemistry

The synthesis of the desamino analogue **1** of m-NBA has been described previously.[23] Isoxazoles **2** and **3** were prepared following the route depicted in Scheme 1. 1.3-Dipolar cycloaddition of hydroxycarboncyanidimic chloride[24] to 3-nitrostyrene yielded the dihydroisoxazole **4**, which was oxidized with NBS to afford upon saponification the restricted rotation analogue **2** of m-NBA and upon treatment with sodium azide its restricted rotation tetrazole bioisostere **3**.

Sulfonamides **5**−**20** were synthesized in a conventional manner, condensing the appropriate arylsulfochloride with 2-amino-4-arylthiazoles (Scheme 2), followed by a deprotection step if necessary, as described in the Experimental Section.

The synthetic access to L-3-bromokynurenine **24**, a convenient precursor for L-[3-^{3}H]kynurenine **25**, has been inspired by the reported synthesis of L-kynurenine[25] and is shown in Scheme 3. The key step involves a Stille-type coupling of (*S*)-3-(benzyloxycarbonyl)-5-oxo-4-oxazolidineacetyl chloride[26] with [2-bromo-6-(trimethylstannanyl)phenyl]carbamic acid *tert*-butyl ester, which was generated in situ from (2,6-dibromophenyl)carbamic acid *tert*-butyl ester **22**. The latter had to be prepared from commercially available 2,6-dibromoaniline via the diphosgene route. Modern protecting group chemistry for the introduction of the Boc group failed due to the steric bulk of the bromine atoms. L-[3-^{3}H]kynurenine **25** was then prepared by catalytic tritiation of **24**.

Scheme 2[a]

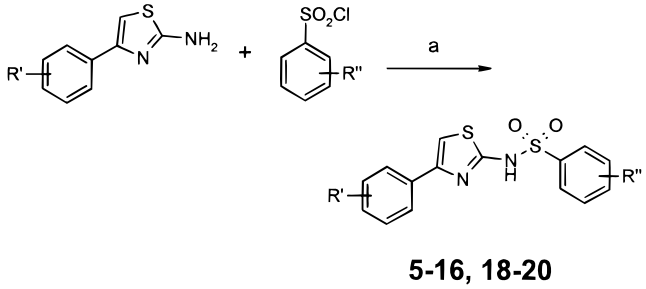

[a] Reagents: (a) pyridine, room temperature.

Scheme 3[a]

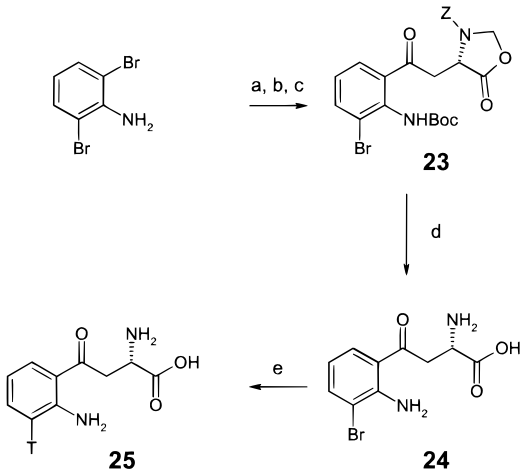

[a] Reagents: (a) diphosgene, toluene, reflux; *tert*-butyl alcohol, reflux; (b) *t*-BuLi, THF, Me_3SnCl, −90 °C; (c) L-4-[(chlorocarbonyl)methyl]-5-oxooxazolidine-3-carboxylic acid benzyl ester, $[Pd_2(dba)_3]CHCl_3$, toluene, 70 °C; (d) 30% HBr in acetic acid; propylene oxide, *i*-PrOH; (e) $^3H_2$, Pd/C (10%), DMF.

Results and Discussion

The compounds described were evaluated in an in vitro enzyme inhibition assay with rat kidney kynurenine 3-hydroxylase using L-[3-^{3}H]kynurenine as substrate. The results are given as IC_{50}'s (concentration required for 50% inhibition) and shown in Tables 1 and 2. Selected compounds were tested in an *ex vivo* enzyme inhibition assay in rat liver and kidney homogenates (Table 3, results as ED_{50}s after oral administration of the test compounds). The extremely low expression level of kynurenine 3-hydroxylase in rat brain hampered the determination of enzyme activity in this tissue. Therefore, *ex vivo* kynurenine 3-hydroxylase inhibition was also measured in gerbils after oral administration. This species has measurable kynurenine 3-hydroxylase activity in the brain. The results obtained in gerbils are displayed in Table 4.

Choosing m-NBA as a lead compound our initial attempt to design new inhibitors focused on one question. Is the relatively low affinity of this compound (IC_{50} = 0.8 μM) an indication that not all functional groups

Table 1. Inhibition of Rat Kidney Kynurenine 3-Hydroxylase by Compounds Related to m-NBA[a]

compd	structure	IC_{50} (nM)
m-NBA	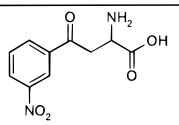	774±113
1	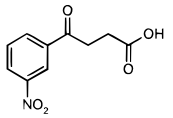	5770±690
2	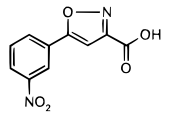	2680±410
3	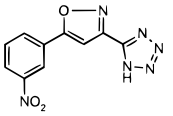	1160±290
5	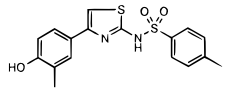	114±20

[a] IC_{50} values were calculated using at least nine inhibitor concentrations. Values are the means ± SEM from three to six experiments, each performed in triplicate.

Table 2. Inhibition of Rat Kidney Kynurenine 3-Hydroxylase[a]

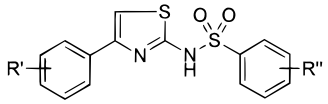

compd	R′	R″	IC_{50} (nM)
6	H	4-Me	470 ± 190
7	4-OMe	4-Me	240 ± 41
8	4-Cl	4-Me	56 ± 8
9	4-Me	4-Me	76 ± 14
10	3-Cl, 4-Cl	4-Me	56 ± 8
11	3-NO_2	4-Me	48 ± 12
12	3-NO_2	H	200 ± 35
13	3-NO_2	3-Cl, 4-Cl	120 ± 36
14	3-NO_2	4-Cl	84 ± 29
15	3-NO_2	4-OMe	51 ± 16
16	3-NO_2	3-OMe, 4-OMe	37 ± 3
17	3-NO_2	4-NH_2	40 ± 3
18	3-NO_2	4-*i*-Pr	990 ± 20
19	2-F, 5-CF_3	3-OMe, 4-OMe	39 ± 17
20	2-F, 5-CF_3	4-NH_2	19 ± 2
m-NBA			774 ± 113
FCE 28833			237 ± 32

[a] IC_{50} values were calculated using at least nine inhibitor concentrations. Values are the means±SEM from three to six experiments, each performed in triplicate.

are involved in binding?[27] The fact that the desamino analogue **1** of m-NBA shows only 1 order of magnitude lower affinity (IC_{50} = 5.7 μM) suggested to us that the amino group while improving affinity is not involved in a salt bridge. Thus the binding motif of substrate type inhibitors may constitute simply of a substituted phenyl ring in the correct orientation and distance to a carboxylic acid function, with one or two heteroatoms as electron-pair donors between the carboxylic acid and the phenyl ring. Isoxazole **2** (IC_{50} = 2.7 μM) supported this hypothesis, providing a simplified non-amino acid structure. However, it still contained the carboxylic acid function which limits optimization of physicochemical parameters for brain penetration. The finding that the carboxylic acid can be replaced by its tetrazole bioisostere, as in **3** (IC_{50} = 1.2 μM), without loss of affinity, turned our attention to sulfonamides as the other classical carboxylic acid bioisosters and led ultimately to the rapid identification of the sulfonamide **5** (IC_{50} = 0.1 μM) from our chemical library.

Table 3. Ex Vivo Inhibition of Kynurenine 3-Hydroxylase Activity in Kidney and Liver from Rats Treated with Various Inhibitors[a]

	ED_{50} (μmol/kg po)	
compd	kidney	liver
16	1.2 (0.8−1.3)	4.7 (3.6−5.6)
19	6.6 (5.4−8.4)	5.3 (4.3−6.9)
20	1.1 (1.0−1.2)	4.6 (4.2−4.9)
15	3.0 (2.4−3.2)	9.0 (5.8−13)
11	13.3 (11.0−15.8)	33.4 (28.6−41.7)
FCE 28833	25.1 (17.1−36.9)	222 (105−466)

[a] The compounds were administered po 2 h before decapitation. ED_{50} values were calculated using six different doses of the inhibitors and four or five animals per group. Values in parentheses represent 95% confidence limits.

Table 4. Ex Vivo Inhibition of Kynurenine 3-Hydroxylase Activity in Brain and Peripheral Organs from Gerbils Treated with Various Inhibitors[a]

	ED_{50} (μmol/kg po)		
compd	brain	kidney	liver
16	5.5 (3.3−9.2)	0.8 (0.5−1.2)	0.4 (0.3−0.5)
19	5.2 (2.9−7.3)	1.8 (1.1−3.2)	0.9 (0.7−1.3)
20	3.0 (1.1−7.8)	0.9 (0.4−1.8)	0.7 (0.3−1.3)
FCE 28833	461 (119−1789)	22.3 (16.9−30.8)	108 (68−173)

[a] The compounds were administered po 2 h before decapitation. ED50 values were calculated using six different doses of the inhibitors and four or five animals per group. Values in parentheses represent 95% confidence limits.

Since sulfonamides were expected to have a superior pharmacological profile with respect to oral bioavailability,[28] further optimization was done on the sulfonamide lead **5**. Examination of the substituent effects[29] in the "western" phenyl ring (compounds **6**−**11**) revealed a preference for lipophilic substituents, one of the best substituents being 3,4-dichloro (**10**) (IC_{50} = 0.06 μM). The high affinity of the 3-nitro compound (**11**) (IC_{50} = 0.05 μM), however, may indicate that these substituents do not target a truly lipophilic site in the enzyme. The high affinity of 3-nitro and 3,4-dichloro compound is a surprising coincidence with the SAR of benzoylalanine-type inhibitors of kynurenine 3-hydroxylase[19,30] and may suggest a common binding site for sulfonamide- and benzoylalanine-type inhibitors. Support for this notion comes from kinetic analysis of the mode of inhibition of **16** (Figure 1) and FCE 28833 (not shown), both of which behaved as competitive inhibitors of kynurenine 3-hydroxylase with K_i values of 4.8 ± 2.1 and 95 ± 27 nM, respectively.

Of the two lead compounds **10** and **11**, only the latter efficiently inhibited the enzyme after oral administration (ED_{50} = 13.3 μmol/kg in the kidney, Table 3). A somewhat higher ED_{50} in the liver (33.4 μmol/kg) may reflect the fact that sulfonamides are cleared mainly via the renal route and thus achieve highest concentration levels in this organ,[31] a property which they seem to share with benzoylalanines such as FCE 28833 (Table 3).

Cursory investigation of the effect of substituents in the "eastern" phenyl ring (compounds **12**−**17,** Table 2)

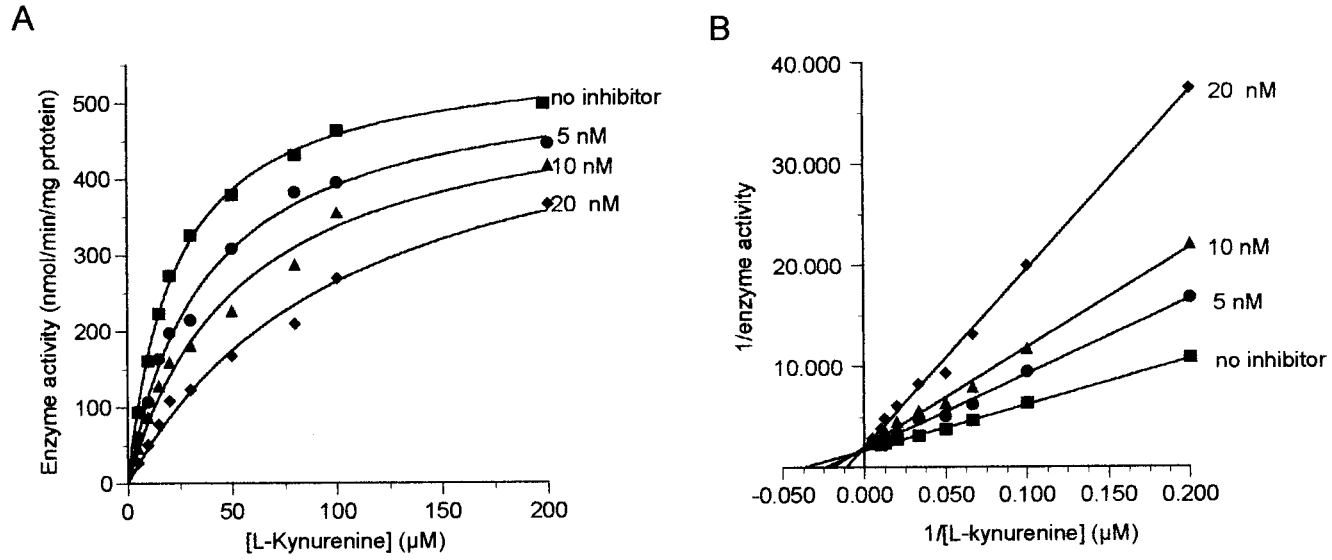

Figure 1. Kinetic analysis of the inhibition of kynurenine 3-hydroxylase in rat kidney mitochondria preparations by various concentrations of **16** (Ro 61-8048). Panel A: saturation analysis. Panel B: double-reciprocal transformation plot of the data. The data shown are representative of three experiments. Note that in this experiment, no preincubation period was performed and the reaction was started by the addition of the enzyme preparation.

revealed that substituents with negative σ-values led to the most potent compounds; however not much difference in IC_{50}'s were found between 4-methyl- (**11**, 0.05 μM), 4-methoxy- (**15**, 0.05 μM), 3,4-dimethoxy- (**16**, 0.04 μM), and 4-amino-substituted compounds (**17**, 0.04 μM). The reason for this poor differentiation is unclear, although it might be due in part to a counterbalancing effect of substituent size, which becomes more evident in the 4-isopropyl compound (**18**, 1.0 μM). While **11**, **15**, and **16** are virtually equipotent in vitro, they differ quite clearly in their efficacy after oral administration (Table 3). With an ED_{50} of 1.2 μmol/kg po in the rat kidney, **16** (Ro 61-8048) is about 10-fold more potent than **11** and about 2-fold more potent than **15** after oral administration.

While **16** achieved our initial goal of developing kynurenine 3-hydroxylase inhibitors well suited for assessing the relevance of the kynurenine pathway in models of neurological damage, this compound is a nitroaromat and thus a potential mutagen. While searching for potential replacements of the 3-nitrophenyl group, we found that a 2-fluoro-5-(triflouromethyl)-phenyl group was a suitable substitute. Compound **20**, which features this substitution pattern on the western phenyl ring, is virtually equipotent to **16** both in vitro (Table 2) and *ex vivo* (Tables 3 and 4).

We have studied the time course of kynurenine 3-hydroxylase inhibition after administration of a single oral dose of **16** in gerbils and rats (Figure 2). In gerbils, a dose of 30 μmol/kg po led to inhibition of the cerebral enzyme which peaked after 2 h (~85% inhibition) and persisted for up to 8 h (Figure 2A). In gerbil kidney and liver this dose of **16** led to >80% inhibition of the enzyme for about 24 h. Recovery of enzyme activity in rats was faster than that observed in gerbils (Figure 2B).

The effect of **16** on the cerebral outflow of KYNA was evaluated in rat hippocampus after implantation of a transversal microdialysis probe (Figure 3). The inhibitor dose-dependently increased the outflow of KYNA, with a single dose of 100 μmol/kg po (42 mg/kg po)

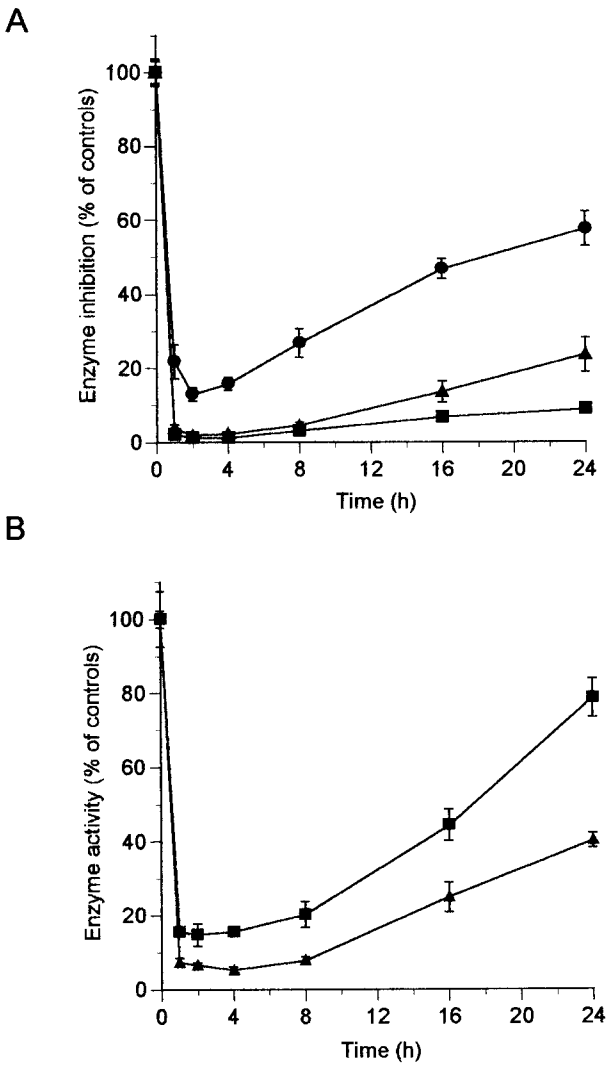

Figure 2. Time course of kynurenine 3-hydroxylase inhibition in homogenates from gerbil (panel A) and rat (panel B) tissues after oral administration of 30 μmol/kg **16** (Ro 61-8048). The data are mean values ± SEM of four or five animals per group: (circle) brain; (triangle) kidney; (square) liver.

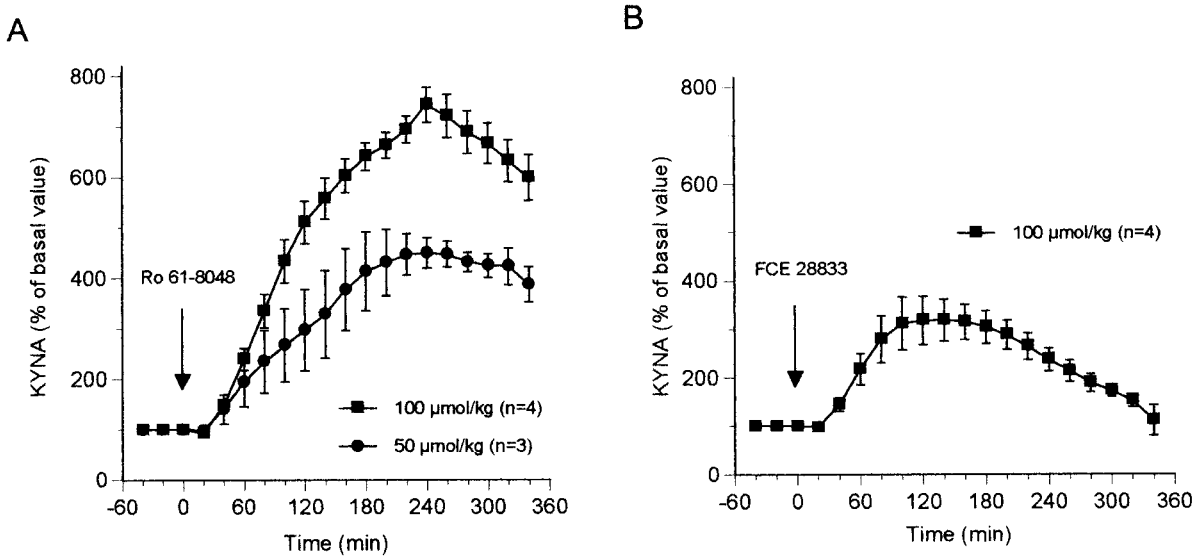

Figure 3. Effect of the kynurenine 3-hydroxylase inhibitors **16** (Ro 61-8048) (panel A) and FCE 28833 (panel B) on KYNA outflow from rat hippocampus. Data are means ± SEM of three or four experiments as indicated in the figure. The basal level of KYNA was 0.22 ± 0.01 pmol/sample (20 μL) corresponding to a concentration of 11.0 ± 0.5 nM (value not corrected for KYNA recovery through the microdialysis probe). No significant changes in KYNA outflow were observed after administration of vehicle solution to the animals.

leading to a concentration of this metabolite 7.5-fold over basal levels. The concentration of KYNA peaked 4 h after oral administration of the compound and remained elevated longer than 6 h. A lower dose (50 μmol/kg po) of **16** led only to a 4-fold increase in KYNA levels, suggesting incomplete inhibition of kynurenine 3-hydroxylase at this dose. At 100 μmol/kg po FCE 28833 produced only a 3-fold increase in KYNA outflow which returned to basal levels after 5 h (Figure 3B). Reports of 8−12-fold increases in rat hippocampal KYNA concentrations have been made with m-NBA at 800 mg/kg ip and FCE 28833 at 400 mg/kg po.[19,21] Given the low levels of kynurenine 3-hydroxylase in rat brain and the massive increase in plasma KYNA,[21] a substantial proportion of the KYNA found in rat hippocampal dialysate may come from the periphery.[32] Thus relevant doses, i.e., doses that might influence brain QUIN concentrations in animal models of neurological damage, might be higher than those needed to elevate brain KYNA concentrations.

Conclusion

We have discovered *N*-(4-phenylthiazol-2-yl)benzenesulfonamides as inhibitors of kynurenine 3-hydroxylase. This novel series of compounds yielded the most potent kynurenine 3-hydroxylase inhibitors known so far, namely 3,4-dimethoxy-*N*-[4-(3-nitrophenyl)thiazol-2-yl]-benzenesulfonamide **16** (IC_{50} = 37 nM, Ro 61-8048) and 4-amino-*N*-[4-[2-fluoro-5-(trifluoromethyl)phenyl]thiazol-2-yl]benzenesulfonamide (**20**) (IC_{50} = 19 nM). These compounds were not only potent in vitro but were also shown to inhibit kynurenine 3-hydroxylase after oral administration, with ED_{50}'s in the range of 3−5 μmol/kg in gerbil brain. **16** (Ro 61-8048) increased kynurenic acid concentration in extracellular hippocampal fluid of rats, and appears to be more potent than FCE 28833. The pharmacological features of the inhibitors described should allow a more detailed investigation of the role of the kynurenine pathway in certain neurological disorders, in particular those associated with neuroinflammation.

Experimental Section

Chemistry. General Procedures. Melting points were taken with a Büchi 535 melting point apparatus and are uncorrected. The ^{1}H spectra were recorded on a Bruker AC250 instrument in DMSO (unless noted otherwise). Low-resolution EI-MS spectra (EI: 70 eV) were recorded on a MS9 updated with a VG ZAB console, Finnigan data system SS300, with direct sample introduction. Microanalysis (C, H, N) were performed on a Heraeus Vario EL. Halogens were determined by standard titrimetric procedures. NMR data are reported in parts per million (δ) relative to internal tetramethylsilane and are referenced to the deuterium lock signal from the sample solvent (d_6-DMSO unless otherwise stated); coupling constants (J) are in hertz. All reactions were performed under argon. Drying of organic solutions was with $MgSO_4$, evaporation in a rotary evaporator at 40 °C in vacuo as appropriate. For chromatography, Merck silica gel 60 (size 70−230 mesh) was used. Analytical TLC plates employed were Merck silica gel 60 F-254 plates. Starting materials were high-grade commercial products unless stated otherwise. The tritiation apparatus was purchased from Radiumchemie AG.[33] Radiochemical samples were counted in a Berthold BF 5020 liquid scintillation counter using Safetron-150 as scintillation cocktail. Counting efficiency was determined by adding [^{3}H]-hexadecane standard (Amersham Radiochemicals) to each sample. The radiochemical purity was determined on a TLC linear analyzer LB284 from Berthold AG. The HPLC apparatus consisted of a Anacomp 220 controller, T114 pump, Uvikon 720 LC detector. The Millex-SR 0.5 μm filter cartridges were obtained from Millipore AG.

5-(3-Nitrophenyl)-4,5-dihydroisoxazole-3-carbonitrile (4). A solution of sodium carbonate in water (40 mL, 0.5 M) was added to a mixture of 3-nitrostyrene (11.1 mL, 80 mmol) and hydroxycarboncyanidimic chloride[24] in diethyl ether (44 mL, 0.9 M) at room temperature. Stirring was continued overnight. The mixture was partitioned between diethyl ether and water. The organic phases were pooled and dried with $MgSO_4$. Evaporation afforded **4** as colorless crystals (4.1 g, 47%); mp 101−103 °C; ^{1}H NMR ($CDCl_3$) 3.22 (dd, J = 8.6, J = 17.4, 1H), 3.75 (dd, J = 11.7, J = 17.4, 1H), 5.97 (dd, J = 8.6, J = 11.7, 1H), 7.66 (m, 2H), 8.19 (bs, 1H), 8.25 (m, 1H). Anal. Calcd ($C_{10}H_7N_3O_3$) C, H, N.

5-(3-Nitrophenyl)isoxazole-3-carboxylic Acid (2). *N*-Bromosuccinimide (2.0 g, 11 mmol) was added to a solution of **4** (2.5 g, 11 mmol) in tetrachloromethane (50 mL). Dibenzoyl peroxide (0.14 g) was added and the mixture boiled overnight. The mixture was cooled to room temperature and filtered and

the filtrate evaporated. Chromatography on silica gel with ethyl acetate/hexanes (1:4) yielded the 5-(3-nitrophenyl)-isoxazole-3-carbonitrile **21** as a beige solid (1.4 g). This solid (0.3 g, 1.4 mmol) was suspended in a mixture of water (10 mL), ethanol (10 mL), and sodium hydroxide solution (28%, 4 mL). The mixture was boiled for 1 h, and ethanol was evaporated. The residue was acidified with HCl and the precipitate collected. Stirring with diethyl ether/*n*-hexane (1:1) yielded **2** as a yellowish solid (0.08 g, 24%): mp >176 °C dec; ^{1}H NMR 7.73 (s, 1H), 7.87 (t, 1H), 8.39 (t, 2H), 8.73 (s, 1H), 13.8 (bs, 1H); MS (high res) mass calcd for $C_{10}H_6N_2O_5$ ($M^{\bullet+}$) = 234.0277; obsd *m*/*z* at 234.0286, deviation from theoretical = 0.9 mmu.

5-[5-(3-Nitrophenyl)isoxazol-3-yl]-1*H*-tetrazole (3). To a solution of **21** (0.8 g, 3.7 mmol) in DMF (10 mL) was added sodium azide (0.3 g, 4.8 mmol) and ammonium chloride (0.26 g, 4.8 mmol). The mixture was stirred for 3 h at 80 °C and cooled to room temperature. Solids were removed by filtration, and the filtrate was evaporated to dryness. The residue was dissolved in water and the product precipitated by addition of HCl. Recrystallization from water/ethanol (1:1) afforded **3** as a beige solid (0.75 g, 79%): mp 228−230 °C; ^{1}H NMR 7.90 (t, 1H), 8.05 (s, 1H), 8.41 (d, 1H), 8.48 (d, 1H), 8.80 (s, 1H), 17.5 (bs, 1H). Anal. Calcd ($C_{10}H_6N_6O_3$) C, H, N.

Preparation of *N*-(4-Phenylthiazol-2-yl)benzenesulfonamides (5−16, 18−19). General Procedure. A mixture of the appropriately substituted 4-arylthiazol-2-ylamine (1.7 mmol) and arylsulfochloride (1.9 mmol) in pyridine (2 mL) was stirred overnight at room temperature. The red solution was poured into 1 N HCl (50 mL). The yellowish precipitate was collected, redissolved in a mixture of ethanol (20 mL) and 2 N NaOH (20 mL), and treated with Norite. Filtration and neutralizing the filtrate with concentrated HCl yielded the product as a powder which was recrystallized from EtOH/water mixtures.

***N*-[4-(4-Hydroxy-3-methylphenyl)thiazol-2-yl]-4-methylbenzenesulfonamide (5):** 0.15 g (25%) of a colorless powder from 50% EtOH; mp 168−170 °C dec; ^{1}H NMR (DMSO) 2.11 (s, 3H), 2.34 (s, 3H), 6.77 (d, 1H), 6.89 (s, 1H), 7.34 (m, 3H), 7.43 (bs, 1H), 7.71 (d, 2H), 9.75 (s, 1H), 13.00 (bs, 1H). Anal. Calcd ($C_{17}H_{16}N_2O_3S_2$) C, H, N, S.

4-Methyl-*N*−(4-phenylthiazol-2-yl)benzenesulfonamide (6):[34] 0.16 g (28%) of a colorless powder from 30% EtOH; mp 152−153 °C. Anal. Calcd ($C_{16}H_{14}N_2O_2S_2$) C, H, N, S.

***N*-[4-(Methoxyphenyl)thiazol-2-yl]-4-methylbenzenesulfonamide (7):** 0.24 g (39%) of a colorless powder from 50% EtOH; mp 85 °C dec; ^{1}H NMR 2.36 (s,3H), 3.78 (s, 3H), 6.99 (d, 2H), 7.03 (s, 1H), 7.35 (d, 2H), 7.64 (d, 2H), 7.73 (d, 2H), 13.2 (bs, 1H). Anal. Calcd ($C_{17}H_{16}N_2O_3S_2$) C, H, N, S.

***N*-[4-(4-Chlorophenyl)thiazol-2-yl]-4-methylbenzenesulfonamide (8):** 0.18 g (28%) of a colorless powder from 40% EtOH; mp 237−239 °C; ^{1}H NMR 2.36 (s, 3H), 7.28 (s, 1H), 7.36 (d, 2H), 7.51 (d, 2H), 7.73 (d, 2H), 7.73 (d, 2H). Anal. Calcd ($C_{16}H_{13}ClN_2O_2S_2$) C, H, N, Cl, S.

4-Methyl-*N*−(4-*p*-tolylthiazol-2-yl)benzenesulfonamide (9): 0.46 g (78%) of a beige powder from 50% EtOH; mp 186 °C dec; ^{1}H NMR 2.31 (s, 3H), 2.36 (s, 3H), 7.13 (s, 1H), 7.24 (d, 2H), 7.35 (d, 2H), 7.59 (d, 2H), 7.73 (d, 2H), 13.15 (s, 1H). Anal. Calcd ($C_{17}H_{16}N_2O_2S_2$) C, H, N, S.

***N*-[4-(3,4-Dichlorophenyl)thiazol-2-yl]-4-methylbenzenesulfonamide (10):** 0.33 g (48%) of a colorless powder from 50% EtOH; mp 205−206 °C; ^{1}H NMR 2.36 (s, 3H), 7.36 (d, 2H), 7.44 (s, 1H), 7.71 (s, 2H), 7.73 (d, 2H), 8.03 (s, 1H), 13.3 (bs, 1H). Anal. Calcd ($C_{16}H_{12}Cl_2N_2O_2S_2$) C, H, N, Cl, S.

4-Methyl-*N*-[4-(3-nitrophenyl)thiazol-2-yl]benzenesulfonamide (11): 0.42 g (62%) of a light yellow powder from 50% EtOH; mp 187−189 °C; ^{1}H NMR 2.36 (s, 3H), 7.37 (d, 2H), 7.58 (bs, 1H), 7.74 (t, 1H), 7.76 (d, 2H), 8.19 (t, 2H), 8.60 (s, 1H). Anal. Calcd ($C_{16}H_{13}N_3O_4S_2$) C, H, N, S.

N-[4-(3-Nitrophenyl)thiazol-2-yl]benzenesulfonamide (12):[34] 0.12 g (20%) of a light yellow powder from 50% EtOH; mp 141−142 °C. Anal. Calcd ($C_{15}H_{11}N_3O_4S_2$) C, H, N, S.

3,4-Dichloro-*N*-[4-(3-nitrophenyl)thiazol-2-yl]benzenesulfonamide (13): 0.30 g (41%) of a light yellow powder from 50% EtOH; mp 189−191 °C; ^{1}H NMR 7.61 (s, 1H), 7.75 (t, 1H), 7.83 (m, 2H), 8.00 (s, 1H), 8.18 (d, 1H), 8.23 (d, 1H), 8.62 (s, 1H), 13.6 (bs, 1H). Anal. Calcd ($C_{15}H_9Cl_2N_3O_4S_2$) C, H, N, Cl, S.

4-Chloro-*N*-[4-(3-nitrophenyl)thiazol-2-yl]benzenesulfonamide (14): 0.43 g (64%) of a yellow powder from 50% EtOH; mp 195−197 °C; ^{1}H NMR 7.59 (s, 1H), 7.65 (d, 2H), 7.74 (t, 1H), 7.87 (d, 2H), 8.18 (d, H), 8.23 (d, 1H), 8.61 (s, 1H), 13.6 (bs, 1H). Anal. Calcd ($C_{15}H_{10}ClN_3O_4S_2$) C, H, N, Cl, S.

4-Methoxy-*N*-[4-(3-nitrophenyl)thiazol-2-yl]benzenesulfonamide (15): 0.31 g (47%) of a yellow powder from 50% EtOH; mp 157−159 °C; ^{1}H NMR 3.82 (s, 3H), 7.09 (d, 2H), 7.58 (bs, 1H), 7.73 (t, 1H), 7.81 (d, 2H), 8.19 (t, 2H), 8.61 (s, 1H), 13.3 (bs, 1H). Anal. Calcd ($C_{16}H_{13}N_3O_5S_2$) C, H, N, S.

3,4-Dimethoxy-*N*-[4-(3-nitrophenyl)thiazol-2-yl]benzenesulfonamide (16): 0.26 g (36%) of a light yellow powder from 70% EtOH; mp 185 °C; ^{1}H NMR 3.81 (s, 6H), 7.10 (d, 1H), 7.32 (s 1H), 7.46 (d, 1H), 7.60 (bs, 1H), 7.73 (t, 1H), 8.19 (t, 2H), 8,60 (s, 1H), 13.3 (bs, 1H). Anal. Calcd ($C_{17}H_{15}N_3O_6S_2$) C, H, N, S.

4-Amino-*N*-[4-(3-nitrophenyl)thiazol-2-yl]benzenesulfonamide (17). Following the general procedure a mixture of 4-(3-nitrophenyl)thiazol-2-ylamine and 4-acetaminobenzenesulfochloride in pyridine yielded 0.60 g of *N*-[4-[[[4-(3-nitrophenyl)thiazol-2-yl]amino]sulfonyl]phenyl]acetamide (**25**) (84%): mp >250 °C; ^{1}H NMR 2.06 (s, 3H), 7.57 (s, 1H), 7.75 (m, 5H), 8.19 (t, 2H), 8.60 (s, 1H), 10.3 (s, 1H), 13.3 (bs, 1H). Anal. Calcd ($C_{17}H_{14}N_4O_5S_2$) C, H, N, S. This material was boiled for 20 h in 6 N HCl (6 mL) and gave upon cooling and recrystallization of the solid precipitate 0.20 g (38%) of a yellow powder from 40% EtOH: mp 191−193 °C; ^{1}H NMR 6.05 (bs, 2H), 6.59 (d, 2H), 7.52 (d, 2H), 7.62 (bs, 1H), 7.72 (t, 1H), 8.19 (d, 2H), 8.60 (s, 1H), 13.0 (bs, 1H). Anal. Calcd ($C_{15}H_{12}N_4O_4S_2$) C, H, N, S.

4-Isopropyl-*N*-[4-(3-nitrophenyl)thiazol-2-yl]benzenesulfonamide (18): 0.19 g (28%) of a light yellow powder from 50% EtOH; mp 144−145 °C; ^{1}H NMR 1.20 (d, 6H), 2.95 (m, 1H), 7.44 (d, 2H), 7.58 (s, 1H), 7.70 (t, 1H), 7.79 (d, 2H), 8.19 (m, 2H), 8.60 (s, 1H), 13.4 (bs, 1H). Anal. Calcd ($C_{18}H_{17}N_3O_4S_2$) C, H, N, S.

***N*-[4-[2-Fluoro-5-(trifluoromethyl)phenyl]thiazol-2-yl]-3,4-dimethoxybenzenesulfonamide (19):** 0.43 g (55%) of a colorless powder from 60% EtOH; mp 126−128 °C; ^{1}H NMR ($CDCl_3$) 3.91 (s, 6H), 6.90 (d, 1H), 7.04 (s, 1H), 7.20 (t, 1H), 7.52 (s, 1H), 7.53 (m, 1H), 7.64 (dd, 1H), 7.83 (dd, 1H), 9.8 (bs, 1H). Anal. Calcd ($C_{18}H_{14}F_4N_2O_4S_2$) C, H, N, F, S.

4-Amino-*N*-[4-[2-fluoro-5-(trifluoromethyl)phenyl]thiazol-2-yl]benzenesulfonamide (20): Following the general procedure a mixture of 4-[2-fluoro-5-(trifluoromethyl)phenyl]-thiazol-2-ylamine and 4-acetaminobenzenesulfochloride in pyridine yielded 0.53 g of *N*-[4-[[[4-[2-fluoro-5-(trifluoromethyl)-phenyl]thiazol-2-yl]amino]sulfonyl]phenyl]acetamide (68%). This material was used without further purification, boiled for 36 h in 6 N HCl (6 mL), and gave upon cooling and recrystallization of the solid precipitate 0.21 g (44%) of a colorless powder from 50% EtOH: mp 107−110 °C; ^{1}H NMR 6.05 (bs, 2H), 6.59 (d, 2H), 7.38 (bs,1H), 7.51 (d, 2H), 7.57 (t, 1H), 7.80 (m, 1H), 8.22 (d, 1H). Anal. Calcd ($C_{16}H_{11}F_4N_3O_2S_2$) C, H, N, F, S.

(2,6-Dibromophenyl)carbamic Acid *tert*-Butyl Ester (22). Diphosgene (21.9 mL, 181 mmol) was added at room temperature to a solution of 2,6-dibromoaniline (37.8 g, 151 mmol) in toluene (400 mL). The mixture was heated slowly to 105 °C and maintained at that temperature for 3 h. (Caution: the reaction is exothermic and started at 80 °C.) After being cooled to room temperature the solution was purged with argon, and the solvent was evaporated. The residue was boiled with *tert*-butyl alcohol (400 mL) for 5 h. The solution was then cooled to room temperature and evaporated to dryness. Chromatography of the residue on silicagel with diethyl ether/hexanes (1:5) afforded **22** as a colorless solid (21.2 g, 40%): mp 103−106 °C; ^{1}H NMR ($CDCl_3$) 1.51 (s, 9H), 6.15 (bs, 1H), 6.99 (t, 1H), 7.57 (d, 2H). Anal. Calcd ($C_{11}H_{13}Br_2NO_2$) C, H, N, Br.

(2S)-4-[2-[3-Bromo-2-[(*tert*-butoxycarbonyl)amino]phenyl]-2-oxoethyl]-5-oxooxazolidine-3-carboxylic Acid Benzyl Ester (23). A solution of **22** (33.8 g, 96 mmol) in THF (700 mL) was cooled to −90 °C. *tert*-Butyllithium (135 mL, 1.5 M) was added, so that the temperature did not rise above −85 °C. Stirring at −90 °C was continued for 2 h, the temperature raised to −75 °C, and trimethyltin chloride (18.7

g, 94 mmol) added. Stirring at −75 °C was continued for 1.5 h and the reaction quenched with water (250 mL). The mixture was partitioned between diethyl ether and water. The organic phases were pooled, washed with brine, and dried with $MgSO_4$. Evaporation of the solvents afforded a yellow oil (33.4 g), containing 50% monotinylated species contaminated with ditinylated compound and starting material.

This oil (33.4 g) was dissolved in toluene (500 mL), (S)-3-(benzyloxycarbonyl)-5-oxo-4-oxazolidineacetyl chloride[26] (23 g, 77 mmol) and tris(dibenzylideneacetone)dipalladium chloroform (0.4 g) were added. The mixture was heated to 70 °C for 4 h, cooled to room temperature, and filtered. The filtrate was partitioned between ethyl acetate and water. The organic phases were pooled and washed with saturated sodium bicarbonate solution and brine. Drying with $MgSO_4$ and evaporation of the solvents yielded a residue which was chromatographed on silica gel with ethyl acetate/hexanes (2:3) to afford **23** as a yellowish foam (6.9 g, 16%): ^{1}H NMR ($CDCl_3$) 1.46 (s, 9H), 3.61 (m, 2H), 4.42 (m, 1H), 5.0−5.6 (m, 4H), 7.0−7.2 (m, 2H), 7.34 (bs, 5H), 7.69 (d, 1H). $[\alpha]^{20}_D$ +89.2 (*c* 1, MeOH); MS (high res) mass calcd for $C_{24}H_{25}BrN_2O_7$ ($M^{\bullet+}$) = 532.0845, obsd *m*/*z* at 532.0846, deviation from theoretical = 0.1 mmu.

(2S)-2-Amino-4-(2-amino-3-bromo-phenyl)-4-oxo-butyric acid (24). 23 (6.0 g, 11.2 mmol) was added to HBr in acetic acid (100 mL, 33%). After 40 min of stirring at room temperature, the mixture was poured into diethyl ether (1.3 L). The hygroscopic precipitate was collected, dried (25 °C/1 mbar), and dissolved in 2-propanol (500 mL). Addition of propylene oxide (5 mL) and stirring for 4 h at room temperature afforded **24** as yellow solid (0.8 g, 25%): mp >175 °C dec; ^{1}H NMR 3.3 (dd, 1H), 3.55 (dd, 1H), 3.7 (m, 1H), 6.57 (t, 1H), 7.22 (bs, 2−3H), 7.68 (d, 1H), 7.81 (d, 1H); $[\alpha]^{20}_D$ −36.0 (*c* 0.5, dioxane/water 1:1); MS (high res) mass calcd for $C_{10}H_{12}BrN_2O_3$ ($M^{\bullet+}$) = 287.00313, obsd *m*/*z* at 287.00324, deviation from theoretical = 0. 11 mmu.

(*S*)-3-[^{3}H]Kynurenine (25). 24 (11.4 mg, 40 μmol) was dissolved in dimethylformamide (6 mL). Dissolution was facilitated by heating and sonication. After filtration of the turbid solution through a Millex-SR 0.5 μm cartridge and addition of 3 mg of 10% Pd on charcoal, the suspension was stirred under tritium gas for 90 min at room temperature. Excess tritium gas was reabsorbed back into the uranium trap and the solvent was lyophilized off by gentle heating with an air blower. then 3 × 3.3 mL of ethanol−water (9/1) were vacuum-transferred into the reaction flask. The suspension was stirred briefly, and the solvent was lyophilized off to remove all volatile tritium activity (2.8 Ci). The vacuum was relieved by nitrogen gas, and the residue was taken up in methanol. After filtration of the catalyst suspension through a Millex-SR 0.5 μm cartridge, the solution was diluted with methanol−toluene (4/1) to 100 mL and stored at −75 °C. The total tritium activity of the crude product was 268 mCi. Half of the crude product was prepurified by chromatography on Amberlite XAD-4. Shortly before use the Amberlite XAD-4 column, 9 × 190 mm was rinsed with 50 mL of ethanol−water (1/1) containing 0.1 mL of concentrated ammonium hydroxide and then with water. Half of the crude product solution was evaporated and redissolved in 10 mL of 0.1 N hydrochloric acid, which was subsequently transferred onto the column. After rinsing with 3 × 2.5 mL of 0.1 N hydrochloric acid and 70 mL of water, **25** was eluted with ethanol−water (1/4). The total tritium activity was 80 mCi. The product was further purified by HPLC using the following conditions: column, Nucleosil 120 C18 5 mm, 4 × 250 mm; mobile phase, buffer−methanol, 3/2; buffer, 50 mM potassium phosphate, pH 5, containing 3 mM; cetyltrimethylammonium bromide; flow rate, 0.8 mL/min, UV detection at 243 nm.

The eluate was lyophilized, and the residue was dissolved in 25 mL of water. This solution was desalted by chromatography on Amberlite XAD-4 as described above. The final product was stored under argon in methanol−toluene (4/1) at −75 °C. The total tritium activity was 64 mCi, and the radiochemical purity was 98% according to TLC (silica gel, 1-butanol−acetic acid−water, 4/1/1). The specific activity was determined by HPLC quantification. Liquid scintillation counting resulted in 14.4 Ci/mmol. This value was consistent with the analysis by mass spectrometry (approximately 50% t_1-species).

Biochemistry. Preparation of Rat Kidney Mitochondria. Rat kidneys were homogenized in 5 volumes of 0.32 M sucrose, buffered to pH 7.4 with 5 mM Tris HCl, containing 0.5 mM phenylmethanesulfonyl fluoride, using a glass−Teflon homogenizer. After centrifugation at 800g for 20 min at 4 °C, the supernatant was collected and recentrifuged at 10000*g* for 20 min at 4 °C. The pellet, consisting of a crude mitochondrial fraction, was rinsed three times with 50 mM potassium phosphate buffer, pH 7.4, containing 0.5 mM EGTA, resuspended in the same buffer and eventually stored in 1 mL aliquots at −80 °C until use.

Protein content was determined using the bicichoninic acid BCA protein assay kit from Pierce.

Kynurenine 3-Hydroxylase Activity Determination and in Vitro Inhibition. Kynurenine 3-hydroxylase activity was measured using a microplate version of the radioenzymatic method described by Erickson et al.,[35] based on the release of tritiated water after hydroxylation of L-[3-^{3}H]-kynurenine (see above). The assay was performed in 96 well/plate in a final volume of 100 μL of 0.1 M potassium phosphate buffer, pH 7.4. The reaction mixture consisted of 100 μM unlabeled L-kynurenine sulfate (Sigma), 0.1 μCi of L-[3-^{3}H]-kynurenine (sp act. 14.4−16.1 Ci/mmol; 1 Ci = 37 GBq), 200 μM NADPH (Boehringer Mannheim), 0.4 unit/mL glucose 6-phosphate dehydrogenase (Boehringer Mannheim), 3 mM glucose 6-phosphate, and 30 μg of the mitochondrial enzyme preparation. In most experiments, a preincubation period of 15 min at 37 °C in the presence of the appropriate concentration of the inhibitor was performed before starting the reaction by the addition of the substrate, and the incubation was prolonged for 10 min at 37 °C. To absorb the unreacted substrate, 150 mL of a 10% (w/v) suspension of activated charcoal (Norit A, Serva) were added to each well, and after shaking for 2 min, the plates were centrifuged for 10 min at 4000 rpm in a Eppendorf model 5403 centrifuge. An aliquot (50 mL) of the samples was then transferred to the well of a second plate, and after addition of 200 μL/well of scintillation fluid (Microscint 40, Packard), sealing, and vigorous shaking for 20 min, the plates were counted for radioactivity using a Top-Count (Packard) counter.

Enzyme activity kinetic constants were calculated by fitting the data obtained from saturation experiments to Michaelis−Menten equation using the Ultrafit (Biosoft) computer program or after Lineweaver−Burke double reciprocal transformation of the data. Inhibition constants (K_i) were calculated from replots of the apparent K_m values versus the inhibitor concentrations used.

Determination of IC_{50} values was performed by fitting the experimental data from inhibition curves using at least eight different inhibitor concentrations to logistic sigmoid equation using a computer program.

Animal Treatment and ex Vivo Inhibition of Kynurenine 3-Hydroxylase Activity in Rat and Gerbils. Male albino rats (120−150 g, RORO) and female gerbils (60−80 g) were obtained from Biological Research Laboratories (Füllinsdorf, Switzerland). Treatment of the animals was performed by oral administration of the compounds (0.5 mL per 100 g of animal weight) at five or six different doses (four or five animals per dose). To ensure the compounds were administered as an homogeneous suspension, they were resuspended in 0.1% Tween-80 in water, homogenized in an all-glass homogenizer, and sonicated in a water-bath sonicator. Control animals were administered with vehicle solution. Two hours after the treatment, the animals were killed by decapitation, and brain, liver, and kidney were rapidly removed. The organs were immediately frozen in dry ice and stored at −80 °C until analysis.

For *ex vivo* kynurenine 3-hydroxylase activity, the tissues were homogenized using a glass−Teflon homogenizer in 9 volumes of 0.32 M sucrose/5 mM Tris-HCl buffer, pH 7.4, containing 0.5 mM phenylmethanesulfonyl fluoride. The enzyme activity was determined using 25 μL of the tissue homogenates as described above except that the incubation

times were 2 min for kidney and liver and 30 min for brain homogenates. ED_{50} values were determined by fitting the data to a logistic sigmoid equation as above.

Microdialysis Technique and Determination of KYNA in Dialysate. Dialysis probes (Filtral 12, AN 69 HF, Hospal Industrie, France) were transversally inserted into the hippocampus of male albino rats (250−300 g) as previously described.[36] After surgery, the animals were allowed to recover for 24 h in their home cages with free access to food and water. The dialysis probes were connected to a microinfusion pump (CMA 100, Schmidlin, Switzerland) and to an electrically actuated injector (Valco, model EC10W). A modified Ringer solution (148 mM NaCl, 5 mM KCl, 1.6 mM $CaCl_2$) was perfused at a flow rate of 2 mL/min through the dialysis probe.

The concentration of KYNA in the dialysate fluid was determined by HPLC with fluorescence detection.[37] The injection of the samples (40 μL) into the HPLC column (Spherisorb ODS2, 125 × 4.6 mm, 3 mm particles; PhaseSep) was controlled by a timer (Valco, Model DVSP4) set to remain in the load position for 20 min and subsequently to the inject position for 5 s. The mobile phase (50 mM sodium acetate buffer, pH 6.2, containing 4.5% acetonitrile) flow rate was 0.75 mL/min. Zinc acetate (0.5 M) was delivered postcolumn at a flow rate of 0.4 mL/min. The fluorescence detector (Merck-Hitachi Model F1080) was set at excitation and emission wavelengths of 344 and 398 nm, respectively.

Acknowledgment. The skillful assistance of B. Frei, R. Wermuth, D. Zimmerli, N. Gebhard, F. D'Agostini, St. Henriot, C. Kuhn, and G. Py is gratefully acknowledged. The authors also thank Drs. W. Arnold, St. MŸller, W. Vetter, Mr. W. Meister, and G. Oesterhelt for spectroscopic determinations and analysis.

References

(1) Rothman, S. M.; Olney, J. W. Excitotoxicity and the NMDA Receptor. *Trends Neurosci.* **1987**, *10*, 299−302 and references therein.

(2) Choi, D. W. Ionic Dependence of Glutamate Neurotoxicity. *J. Neurosci.* **1987**, *7*, 369−379 and references therein.

(3) Monn, J. A.; Schoepp, D. D., Recent Progress in Excitatory Amino Acid Research. *Annu. Rep. Med. Chem.* **1994**, *29*, 53−64 and references therein.

(4) (a) Bender, D. A. Biochemistry of Tryptophan in Health and Disease. *Mol. Aspects Med.* **1982**, *6*, 101−197 and references therein. (b) For a discussion of the relevance of the kynurenine pathway and its metabolites in disease see: refs 8, 19, and 20.

(5) Stone, T. W.; Perkins, M. N. Actions of Excitatory Amino Acids and Kynurenic Acid in the Primate Hippocampus: a Preliminary Study. *Neurosci. Lett.* **1984**, *52*, 335−340.

(6) Kessler M.; Terramani, T.; Lynch, G.; Baudry, M. A Glycine Site Associated with *N*-Methyl-D-aspartic Acid Receptors. Characterization and Identification of a New Class of Antagonists. *J. Neurochem.* **1989**, *52*, 1319−1328.

(7) Saito, K.; Nowak, T. S.; Markey, S. P.; Heyes, M. P. Mechanism of Delayed Increases in Kynurenine Pathway Metabolism in Damaged Brain Regions Following Transient Cerebral Ischemia. *J. Neurochem.* **1993**, *60*, 180−192.

(8) Reinhard, J. F., Jr.; Erickson, J. B.; Flanagan, E. M. Quinolinic Acid in Neurological Disease: Opportunities for Novel Drug Discovery. *Adv. Pharmacol.* **1994**, *30*, 85−125 and references therein.

(9) Takikawa, O.; Yoshida, R.; Kido, R.; Hayashi, O. Tryptophan Degradation in Mice Initiated by Indoleamine 2,3-dioxygenase. *J. Biol. Chem.* **1986**, *261*, 3648−3653.

(10) Saito, K.; Nowak, T. S.; Suyama, K.; Quearry, B. J.; Saito, M.; Crowley, J. S.; Markey, S. P.; Heyes, M. P. Kynurenine Pathway Enzymes in Brain: Responses to Ischemic Brain Injury Versus Systemic Immune Activation. *J. Neurochem.* **1993**, *61*, 2061−2070.

(11) Heyes, M. P.; Saito, K.; Markey, S. P. Human Macrophages Convert L-Tryptophan into the Neurotoxin Quinolinic Acid. *Biochem. J.* **1992**, *283*, 633−635.

(12) Heyes, M. P.; Achim, C. L.; Wiley: A. A.; Major, E. O.; Saito, K; Markey, S. P. Human microglial convert L-tryptophan into the neurotoxin quinolinic acid. *Biochem. J.* **1996** *320*, 595−597.

(13) Yoshitatsu, S.; Paul, I. A.; Saito, K.; Layar, R.; Hartley, J. W.; Morse III, H. C.; Skolnick, P.; Heyes, M. P. Quinolinic Acid Levels in a Murine Retrovirus-Induced Immunodeficiency Syndrome. *J. Neurochem.* **1996**, *66*, 296−302.

(14) Blight, A. R.; Cohen, T. I.; Saito, K.; Heyes, M. P. Quinolinic Acid Accumulation and Functional Deficits Following Experimental Spinal Cord Injury. *Brain* **1995**, *118*, 735−752.

(15) Flanagan, E. M.; Erickson, J. B.; Viveros, H.; Chang, S. Y.; Reinhard, J. F., Jr. Neurotoxin Quinolinic Acid is Selectively Elevated in Spinal Cords of Rats with Experimental Allergic Encephalomyelitis. *J. Neurochem.* **1995**, *64*, 1192−1196.

(16) Whetsell, W. O. J.; Schwarcz, R. Prolonged Exposure to Submicromolar Concentrations of Quinolinic Acid Causes Excitotoxic Damage in Organotypic Cultures of Rat Corticostriatal System. *Neurosci. Lett.* **1989**, *97*, 271−275.

(17) Schurr, A.; West, C. A.; Rigor, B. M. Neurotoxicity of Quinolinic Acid and its Derivatives in Hypoxic Rat Hippocampal Slices. *Brain Res.* **1991**, *568*, 199−204.

(18) Schurr, A.; Payne, R. S.; Heine, M. F.; Rigor, B. Hypoxia, Excitotoxicity, and Neuroprotection in the Hippocampal Slice Preparation. *J. Neurosci. Methods* **1995**, *59*, 129−138.

(19) Pellicciari, R.; Natalini, B.; Constantino, G.; Mahmoud R. M.; Mattoli, L.; Sadeghpour, B. M.; Moroni, F.; Chiarugi, A.; Carpenedo, R. Modulation of the Kynurenine Pathway in Search for New Neuroprotective Agents. Synthesis and Preliminary Evaluation of (*m*-Nitrobenzoyl)alanine, a Potent Inhibitor of Kynurenine-3-Hydroxylase. *J. Med. Chem.* **1994**, *37*, 647−655.

(20) Carpenedo, R.; Chiarugi, A.; Russi, P.; Lombardi, G.; Carla, V.; Pellicciari, R.; Mattoli, L.; Moroni, F. Inhibitors of Kynurenine Hydroxylase and Kynureninase Increase Cerebral Formation of Kynurenate and have Sedative and Anticonvulsant Properties. *Neuroscience* **1994**, *61*, 237−244.

(21) Speciale, C.; Cini, M.; Wu, H.-Q.; Salvati, P.; Schwarcz, R.; Molinari, A.; Calabresi, M.; Varasi, M. Kynurenic acid-enhancing and anti-ischemic effects of the potent kynurenine 3-hydroxylase inhibitor FCE 28833 in rodents. *Adv. Exp. Med. Biol.* **1996**, *398*, 221−227.

(22) Alberati-Giani, D.; Cesura, A. M.; Broger, C.; Warren, W. D.; Röver, S.; Malherbe, P. Cloning and functional expression of human kynurenine 3-monooxygenase. *FEBS Lett.* **1997**, *410*, 407−412.

(23) Roy, K.; Srivastava, R. P.; Tekwani, B. L.; Pandey, V. C.; Bhaduri, A. P. Synthesis and Exploration of New Biological Activities in Ethyl 6/7-Substituted and 6,7-Disubstituted Quinolin-4-One-3-Carboxylates. *Bioorg. Med. Chem. Lett.* **1996**, *6*, 121−126.

(24) Kozikowski, A. P.; Adamczyk, M. Methods for the Stereoselective Cis Cyanohydroxylation and Carboxyhydroxylation of Olefins. *J. Org. Chem.* **1983**, *48*, 366−372.

(25) Salituro, F. G.; MacDonald, I. A. Facile Synthesis of L-Kynurenine. *J. Org. Chem.* **1988**, *53*, 6138−6139.

(26) Hsiao, C.-N.; Leanna, M. R.; Bhagavatula, L.; De Lara, E.; Zydowsky, T. M.; Horrom, B. W.; Morton H. E. Synthesis of N-(*t*-Butoxycarbonyl)-3-(4-Thiazolyl)-L-Alanine. *Synth. Commun.* **1990**, *20*, 3507−3517.

(27) Andrews, P. R.; Craik, D. J.; Martin J. L. Functional Group Contributions to Drug-Receptor Interactions. *J. Med. Chem.* **1984**, *27*, 1648−1657.

(28) Atef, M.; Youssef, A. H.; Ramadan, A.; Issa, M. Kinetic Disposition, Systemic Bioavailability and Acetylation of Some Sulphonamides in Goats. *Arch. Int. Pharmacodyn.* **1989**, *302*, 27−39.

(29) Topliss, J. G. A Manual Method for Applying the Hansch Approach to Drug Design. *J. Med. Chem.* **1977**, *20*, 463−469.

(30) Giordani, A.; Corti, L.; Cini, M.; Marconi, A.; Pillan, A.; Ferrario, R.; Schwarcz, R.; Guidetti, P.; Speciale, C.; Varasi, M. Benzoylalanine Analogues as Inhibitors of Rat Brain Kynureninase and Kynurenine 3-Hydroxylase. In *Recent Advances in Tryptophan Research*; Filippini, G. A., Costa, C. V., Bertazzo, A., Eds.; Plenum Press: New York, 1996; pp 499−505.

(31) Sammes, P. G. Sulfonamides and Sulfones. In *Comprehensive Medicinal Chemistry Vol. 2*; Hansch, C., Sammes, P. G., Taylor, J. B., Eds.; Pergamon: Oxford, 1990; pp 255−270.

(32) Lou, G. L.; Pinsky, C.; Sitar, D. S. Kynurenic Acid Distribution into Brain and Peripheral Tissues of Mice. *Can. J. Physiol. Pharmacol.* **1994**, *72*, 161−167.

(33) Eberle, A. N.; Zeller, A. Tritiation of peptides to high specific radioactivity. Part 1. Synthesis and Biological Properties of [13-($^3H_4$)Norvaline]-α-MSH and of [2,23-bis($^3H_2$)Tyrosine)]ACTH(1−24). *Helv. Chim. Acta* **1985**, *68*, 1880−92.

(34) Vanmaele, L. Dye Donor Element for Use in a Thermal Dye Transfer Method. Eur. Pat. Appl., EP 687573 A1 951220.

(35) Erickson, J. B.; Flanagan, E. M.; Russo, S.; Reinhard, J. F., Jr. A Radiometric Assay for Kynurenine 3-Hydroxylase Based on the Release of ^3H_2O During Hydroxylation of L-[3,5-^{3}H]-Kynurenine. *Anal. Biochem.* **1992**, *205*, 257−262.

(36) Colzi, A; D'Agostini, F.; Cesura, A. M.; Borroni, E.; Da Prada, M. Monoamine oxidase-A inhibitors and dopamine metabolism in rat caudatus: Evidence that an increased cytosolic level of dopamine displaces reversible monoamine oxidase-A inhibitors in vivo. *J. Pharmacol. Exp. Ther.* **1993**, *265*, 103−111.

(37) Swartz, K. J.; During, M. J.; Freese, A.; Beal M. F. Cerebral Synthesis and Release of Kynurenic Acid: An Endogenous Antagonist of Excitatory Amino Acid Receptors. *J. Neurosci.* **1990**, *10*, 2965−2973.

JM970467T